Research Paper

Effect of Particle Size and Compression Force on Compaction Behavior and Derived Mathematical Parameters of Compressibility

Sarsvatkumar Patel,[1] Aditya Mohan Kaushal,[1] and Arvind Kumar Bansal[1,2]

Purpose. To analyze the influence of inherent densification and deformation properties of paracetamol on the mathematical parameters derived from Heckel, Walker, Kawakita, and Adams equations and to correlate these with single particle nominal fracture strength and bulk compression parameters using confined compression on a fully instrumented rotary tablet press.

Materials and Methods. Force–displacement data were captured during in-die compression for four different particle size fractions (150–250, 300–450, 500–650, and 700–1,000 μm) of paracetamol each at compression force of 5.2, 8.6, and 17.3 kN. Nominal single particle fracture strength was obtained by micro tensile testing.

Results. Apparent mean yield pressure (Py) from Heckel analysis was significantly affected by the applied pressure, and was influenced by elastic energy and Young's modulus. The single particle fracture strength correlated to parameters obtained from Heckel, Walker, Kawakita, and Adams equations. Results obtained from bulk compression and single particle measurements were consistent with, and polynomially related to Py, Kawakita ($1/b$), and Adams parameter (τ_0').

Conclusions. Values of Py, $1/b$, and τ_0' obtained from Heckel, Kawakita, and Adams equations, respectively, can be interpreted as a measure of single particle nominal fracture strength during confined compression loading. Walker and Adams parameters were less affected, than Heckel and Kawakita parameters, by the applied pressure.

KEY WORDS: Adams equation; compaction; elastic recovery; Heckel equation; Kawakita equation; Walker equation.

INTRODUCTION

Mechanical properties of single particles or agglomerates influence a number of pharmaceutical unit operations like size reduction, handling, and compression. It has been emphasized that resistance to deformation of bulk material is related to ultimate yield strength of particle undergoing compaction (1). Attempts have been made to infer the single particle properties based on macroscopic observations (bulk compression) such as the variation of the pressure with volume, density, and strain of particulate bed. Compression of a bed of agglomerates/system of particles in a confined space gives the strength of an agglomerate/particle, estimated from the in-die measurement of applied stress and strain (2). Although the compaction process is difficult to analyze, attempts to ascribe a meaning to the various parameters obtained from mathematical models can be helpful in understanding the compaction process. It is therefore of great interest to elucidate what exactly the mathematical models provide with critical consideration to material's dominant deformation behavior under pressure.

Over the years, a number of mathematical models have been proposed to describe the compaction data and understand the inherent compaction behavior under pressure. The first accurate compaction data were probably obtained by Walker (3). Shapiro (4) proposed a model for the reduction of porosity of a bed during compaction in the form of a first order rate process relating the pressure to the porosity. Later, Heckel (5,6) plotted the experimental data on the compaction of metal powders based on Shapiro's model, which describes the data of relative tablet density against compaction pressure, and assumes that the rate of change in density with respect to pressure is directly proportional to the remaining porosity. Another model proposed by Kawakita (7,8) described the course of volume reduction as a function of applied pressure, and is based on the assumption of parallel columns for force transmission. Relationship between pressure on the bed and natural strain was put forth by Adams *et al.* (2).

Various studies have discussed the limitations of Heckel parameter to describe compaction process because the true density, compacted mass, and elastic recovery affect the calculated parameters from Heckel equation (9–12). The data discrimination between material's compaction behaviors

---

[1] Department of Pharmaceutical Technology (Formulations), National Institute of Pharmaceutical Education and Research (NIPER), S.A.S. Nagar, Punjab 160 062, India.

[2] To whom correspondence should be addressed. (e-mail: akbansal@niper.ac.in)

is improved if the compression data are fitted in the form of the Walker model (13). An interesting study by Hassanpour *et al.* reported use of simulated approach with distinct elemental analysis of Heckel model of powder compression and comparison with experimental parameters (14). Nicklasson (15) reported the analysis of the compression mechanics of pharmaceutical agglomerates of different porosity and composition using the Adams and Kawakita equations and interpreted the values of derived constant as a measure of agglomerate strength. Attempts have also been made to describe the entire compression profile in distinct parts by several equations (16) or with a polynomial with several coefficients (17). Panelli *et al.* (18), (density *versus* square root of pressure), Sonnergaard (log–exp model) (19), and Picker (3-D model for densification) (20) are some of the other theoretical models to fit compaction data and improve the predictability of compaction process.

Initial particle rearrangement, fragmentation and viscoelastic deformation of the particles have a significant effect on the derived compaction behavior. Elastic deformation contributes significantly as the porosity decreases below 5 to 10%, where the properties of the compact start to resemble those of the solid-nonporous material. For softer materials, such as pharmaceuticals and other organic materials, that have a low Young's moduli, elasticity is significant at higher pressures. The tablet density changes at different rates during different phases of compression, and various stages of compression (initial particle rearrangement, viscoelastic phase, and strain hardening) overlap in a single compaction event (10). This makes it difficult or impossible to point out distinct regions where only one type of deformation-plastic, elastic or brittle occurs (13). Moreover, there is an effect of initial particle rearrangement or deformation on the overall yield strength of materials. There is a lack of literature on interrelation between the various mathematical models and the influence of the material's inherent deformation properties on the derived constants. Different models are based on varying assumptions, and therefore there is a need to evaluate the ability of parameters derived from different models in elucidating the densification. The present study assesses the discriminative power of various mathematical models of densification, with respect to initial phase of particle rearrangement, effect of applied force (pressure dependency), density change, and elastic properties (elastic deformation and Young's modulus). Paracetamol, a poorly compressible drug with high elastic deformation was chosen for this study (21–23). A range of particle sizes, and varying compression forces have been used to study the compaction behavior. Compression studies have been done on a fully instrumented rotary tableting machine that allows study of basic stress–strain relationship, with respect to actual tableting condition (24).

MATERIALS AND METHODS

Paracetamol

Paracetamol was gifted by Arbro Pharmaceuticals Ltd., New Delhi. Four different particle size ranges; 700–1,000, 500–650, 300–450, and 150–250 μm were obtained by sieving from the bulk material.

Powder X-Ray Diffraction (PXRD)

PXRD of as received paracetamol was recorded under ambient conditions on X-ray powder diffractometer, (D8 Advance, Bruker, Karlsruhe, Germany) using Cu Kα radiation (=1.54 Å) at 40 kV, 40 mA passed through nickel filter.

Differential Scanning Calorimetry (DSC)

DSC of paracetamol was done using DSC (Diamond DSC, Perkin Elmer, Shelton, CT, USA). Temperature axis and the cell constant were calibrated using ultra pure indium. Drug sample (4–6 mg) was weighed and analyzed in pinholed aluminum pans at a heating rate of 10°C/min; over a temperature range of 25 to 200°C under nitrogen purge of 20 ml/min. Melting point and enthalpy values were obtained from the thermogram.

True Density and Particle Size Measurement

The true density was determined in triplicate by helium pycnometry (Pycno 30, Smart Instruments, Mumbai, India) at ambient conditions. Median particle size was determined by optical microscopy by measuring diameter along the longest axis for at least 300 particles (DMLP microscope, Leica Microsystems, Wetzlar, Germany).

Single Particle Fracture Strength

The measurement of single particle nominal fracture strength were performed using a texture analyzer (TA-XT2i, Stable Micro Systems, Surrey, UK), which was calibrated for both the distance and the load cell. All experiments were done with 5 kg load cell and 2 mm flat faced probe. The force required to travel a specified distance was measured as the fracture force of an individual particle. Instrument parameters were fixed as; pre test speed of 0.4 mm/s, test speed of 0.2 mm/s (fracture speed), and post test speed of 0.6 mm/s; and the data acquisition rate was 200 points per second using fully integrated data acquisition and analysis software (Texture Expert, version 1.22). A stainless steel support was kept on platform to support the test particle so it could be axially aligned to the probe. The probe was vertically moved down on single particle until it was observed to fracture. Fracture strength of 20 single particles from each of the four particle ranges was measured at ambient conditions.

Tableting and Data Acquisition

Rotary tablet press (Mini II, Rimek, Ahmedabad, India) was equipped at one of the eight stations with 8 mm D-tooling with flat punch tip. Feed frame was used for uniform die filling and blind dies were used at all other positions. Precompression rollers were set out of function. Tablet weight was kept constant at 202 ± 3 mg and applied force was leveled by moving the pressure roller with a hand wheel. Humidity ($40 \pm 5\%$ RH) and temperature ($25 \pm 5°C$) conditions were controlled throughout the study. Each of the four particle size ranges was compressed at three different forces of 5.2 (0.4), 8.6 (0.3), 17.3 (1.6) kN.
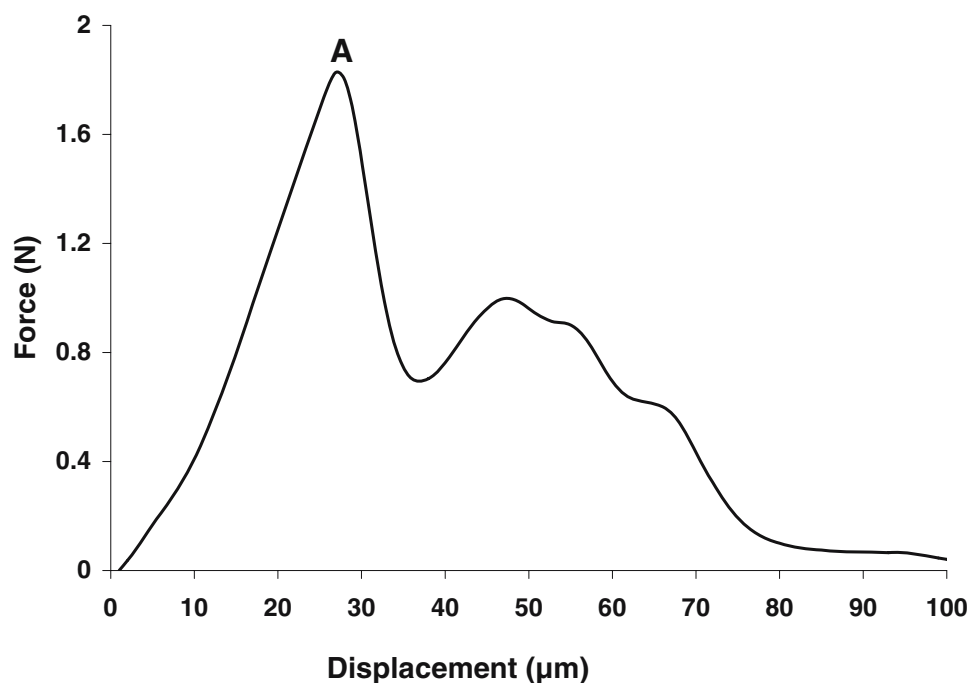
Fig. 1. Representative force–displacement plot for calculating the nominal fracture strength by micro tensile testing. Peak value *A* was taken for calculations.

Data was acquired by Portable Press Analyzer™ (PPA) version 1.2, revision D (Data Acquisition and Analyzing System, PuuMan Oy, Kuopio, Finland), through an infrared (IR) telemetric device with 16-bit analog-to-digital converter (6 kHZ). Force was measured by strain gauges at upper and lower punches (350 Ω, full Wheatstone bridge; I. Holland Tableting Science, Nottingham, UK), which were coupled with displacement transducers (linear potentiometer, 1,000 Ω). Upper and lower punch data were recorded and transmitted on separate channels by individual amplifiers ("Boomerangs"). The amplifiers truncated the raw data from 16 bit to 12 bit after measuring to check IR transmission (data transmission rate—50 kbaud; Internal data buffer—1,024 measurement points). Analysis of compaction data was carried out by PPA Analyse software (version 1.2, revision D). Accuracy of force and displacement transducers was 1 and 0.02%, respectively. The suitability of the data acquisition system has previously been reported (25).

Statistical Analysis

SigmaStat® version 2.03, Systat Software Inc. SPSS Ltd. (Hong Kong) was employed for all regression analysis. Design Expert® version 6.0.8, Stat-Ease Inc. (Minneapolis, USA) was employed for response surface analysis.

RESULTS

Characterization of Paracetamol

PXRD of paracetamol gave a diffractogram with sharp peaks, matching those of the monoclinic (Form I) polymorph of paracetamol (26,27). Melting onset temperature (173.8°C) and fusion enthalpy value (177.8 J/g) further confirmed the monoclinic form. True density value (*n* = 3) was found to be 1.2947 ± 0.0002, which was in close agreement to the earlier reports on true density calculated from crystal structure of monoclinic form (26).

Single Particle Fracture Strength

A distinct force maximum in force–displacement profile was observed, that corresponded to the point at which the test particle was observed to fracture (Fig. 1). The nominal fracture strength, (τ_{0s}) for each particle was calculated from the maximum force using the following expression:

$$\tau_{0_S} = 4F_{max}/\pi d^2 \tag{1}$$

where, F_{max} is the maximum observed fracture force, and *d* is the median diameter (in mm) of the particle undergoing test. Average nominal fracture strength varied from 41.9 N/mm^2 for 150–250 µm particles to 3.3 N/mm^2 for 700–1,000 µm particles (Table I).

Table I. Median Particle Size and Nominal Fracture Strength for Different Sized Particles

Particle size (µm)	Median particle size (µm)	Nominal fracture strength range (N/mm^2)	Average nominal fracture strength (N/mm^2)
700–1,000	860	2.3–4.96	3.3 (0.8)
500–650	550	5.39–8.56	6.9 (0.9)
300–450	380	13.45–15.83	16.4 (4.0)
150–250	210	32.32–59.2	41.9 (8.8)

Values in parenthesis indicate standard deviations.

Mathematical Analysis of Compaction Data

Compression of all four particle size fractions of paracetamol at the studied compression forces (5.2, 8.6, 17.3 kN) gave extremely weak tablets with no measurable tensile strength indicating very weak interparticulate bonding between particles. Force displacement compression profile obtained from the instrumented tableting press was mathematically transformed to fit Heckel, Walker, Kawakita, and Adams equations.

Heckel Analysis

The Heckel model (5,6) provides a method for transforming a parametric view of the force and displacement signals to a linear relationship for materials undergoing compaction. The equation is based on the assumption that the dependence of densification on pressure is of first-order.

$$In[1/1 - D] = KP + A \qquad (2)$$

where, D is the relative density of the tablet (the ratio of tablet density to true density of powder) at applied pressure P, and K is the material-dependent constant i.e., the slope of the straight line portion of the Heckel plot and the reciprocal of K is the mean yield pressure. In-die measurements of the tablet thickness give apparent mean yield pressure (Py). Constant A gives densification of the powder due to initial particle rearrangement, (D_a). A being the sum of two densification terms:

$$A = In[1/1 - D_0] + B \qquad (3)$$

where, ln $[1/1 - D_0]$ is related to the initial die filling and B gives densification due to slippage and rearrangement of primary and fragmented particles, (D_b). D_0 is defined as the densification due to die filling or initial powder packing.

$$D_a = 1 - e^{-A} \qquad (4)$$

$$D_b = D_a - D_0 \qquad (5)$$

For studying the effect of compression force and particle size on derived Heckel parameters, linear regression was done on straight line portions of the Heckel plot between 25 and 90 MPa ($R^2 > 0.99$ in all cases). The parameters obtained from Heckel analysis of the four particle size ranges each at three compression forces along with the Young's moduli are summarized in Table II. Heckel analysis showed that for a given pressure, as the particle size increased, values of relative densities increased. Hence, a higher degree of densification was exhibited by the larger particles as compared to smaller particles and the values of Py were higher for smaller sized particle fraction at all compression forces. For a given size fraction of paracetamol, the apparent mean yield pressure increased with an increase in the compression force. The values of D_0, D_a and D_b obtained from initial region (0–25 MPa, Fig. 2) decreased with decreasing particle size thereby indicating a higher propensity for particle rearrangement and/or fragmentation in case of larger sized particles at a given pressure.

Walker Analysis

The compression data were analyzed by Walker equation (3) in order to study the course of volume reduction. The Walker equation is based on the assumption that the rate of change of volume is proportional to the applied pressure.

$$\log P = -L \times V'/V_0 + C_1 \qquad (6)$$

where, V_0 is the volume at zero porosity and V' is the volume at pressure P. The relative volume is $V'/V_0 = V = 1/D$. The coefficient L is referred to as the pressing modulus and C_1 is a constant. Value of pressing modulus increased as the particle size increased. Walker also proposed another equation in terms of the percentage relative volume as the dependent variable.

$$100V = -W \log P + C \qquad (7)$$

where, W (compressibility coefficient) expresses the percent change in volume of the material when the pressure is increased on log scale, and is considered as a measure of the irreversible compressibility of the compact. C is a constant. Table III represents the results of pressing modulus, L and compressibility coefficient, W from the linear regression analysis of log P vs. $1/D$ (V'/V_0) and $100V$ vs. log P between pressure ranges from 5 to 125 MPa. Results indicate that as the particle size decreased, W increased.

Kawakita Analysis

The basis for the Kawakita equation for powder compression is that the particles subjected to compressive load are in equilibrium at all stages of compression, so that the product of pressure term and volume term is constant (7,8). The Kawakita equation is:

$$P/C = [P/a + 1/ab] \qquad (8)$$

$$C = [(V_0 - V)/V_0] \qquad (9)$$

where, P is the applied axial pressure, and a is the value of initial porosity which corresponds to the total portion of reducible volume at maximum pressure. Mathematically, $1/b$ is simply the pressure needed to compress the powder to one half of the total volume reduction estimated as a term. b is proposed to be inversely related to the yield strength of particles (15). C is the degree of volume reduction, V is volume of compact at pressure P, and V_0 is the initial apparent volume of powder.

Results from the Kawakita modeling of compaction data for different sized fraction are described in Table III. Parameter a decreased with a decrease in particle size and an increase in compression pressure. The parameter $1/b$, which describes the yield strength increase with a decrease in particle size and with an increase in compression pressure. However, at the highest compression force studied (17.3 kN), no visible trend in $1/b$ was observed.

Table II. Apparent Mean Yield Pressure (Py), Densification Due to Initial Particle Rearrangement (D_a), Densification Due to Initial Die Filling (D_0), and Densification Due to Slippage and Rearrangement of Primary and Fragmented Particles (D_b) Obtained from In-die Heckel Analysis for Four Particle Size Fractions of Paracetamol at Three Different Compression Forces

Compression force (kN)	Particle size (μm)	Py (MPa)	D_a	D_0	D_b	Young's Moduli (GPa)	Elastic recovery (ER)	EE/PE ratio
5.2 (0.4)	700–1,000	70.8 (4.7)	0.796 (0.004)	0.625 (0.006)	0.171 (0.004)	1.60 (0.20)	0.03 (0.024)	0.005 (0.00023)
	500–650	81.5 (1.0)	0.783 (0.002)	0.624 (0.004)	0.159 (0.002)	1.25 (0.06)	0.01 (0.0002)	0.0008 (0.00015)
	300–450	87.3 (3.6)	0.764 (0.003)	0.610 (0.005)	0.153 (0.003)	1.15 (0.07)	0.01 (0.0003)	0.00065 (0.0005)
	150–250	96.9 (3.8)	0.746 (0.004)	0.595 (0.005)	0.151 (0.003)	1.08 (0.01)	<0.01 (0.0001)	0.0004 (0.0003)
8.6 (0.3)	700–1,000	93.1 (3.0)	0.766 (0.003)	0.616 (0.004)	0.150 (0.002)	2.13 (0.07)	1.10 (0.01)	0.0055 (0.0005)
	500–650	100.7 (2.0)	0.760 (0.002)	0.612 (0.003)	0.148 (0.003)	2.04 (0.06)	1.06 (0.012)	0.0038 (0.0006)
	300–450	102.5 (3.7)	0.749 (0.004)	0.603 (0.005)	0.146 (0.003)	1.92 (0.02)	1.02 (0.05)	0.0034 (0.00056)
	150–250	129.9 (3.2)	0.711 (0.003)	0.566 (0.006)	0.145 (0.004)	1.89 (0.01)	1.00 (0.044)	0.003 (0.00066)
17.3 (1.6)	700–1,000	118.2 (4.4)	0.771 (0.003)	0.599 (0.004)	0.172 (0.003)	4.85 (0.80)	4.12 (0.38)	0.0131 (0.0022)
	500–650	135.7 (6.6)	0.770 (0.005)	0.593 (0.055)	0.177 (0.055)	3.68 (0.30)	3.50 (0.45)	0.0098 (0.0033)
	300–450	176.8 (13.7)	0.741 (0.017)	0.566 (0.006)	0.174 (0.020)	2.92 (0.06)	3.04 (0.27)	0.006 (0.0017)
	150–250	201.6 (8.3)	0.772 (0.005)	0.606 (0.006)	0.166 (0.005)	2.88 (0.30)	2.40 (0.27)	0.00445 (0.0004)

Values of D_a, D_0, and D_b are derived from initial part of Heckel plot (0–25 MPa, $0.92 < R^2 > 0.96$) and Py is derivative of inverse slope value from regression analysis of linear portion (25–90 MPa, $R^2 > 0.99$), below the relative density of 0.93. Elastic recovery (ER), elastic energy/plastic energy ratio (EE/PE) and Young's moduli calculated from the gradient of stress and strain relationship for each data set are shown. Each value represents an average of six tablet measurements with their standard deviations in parenthesis.
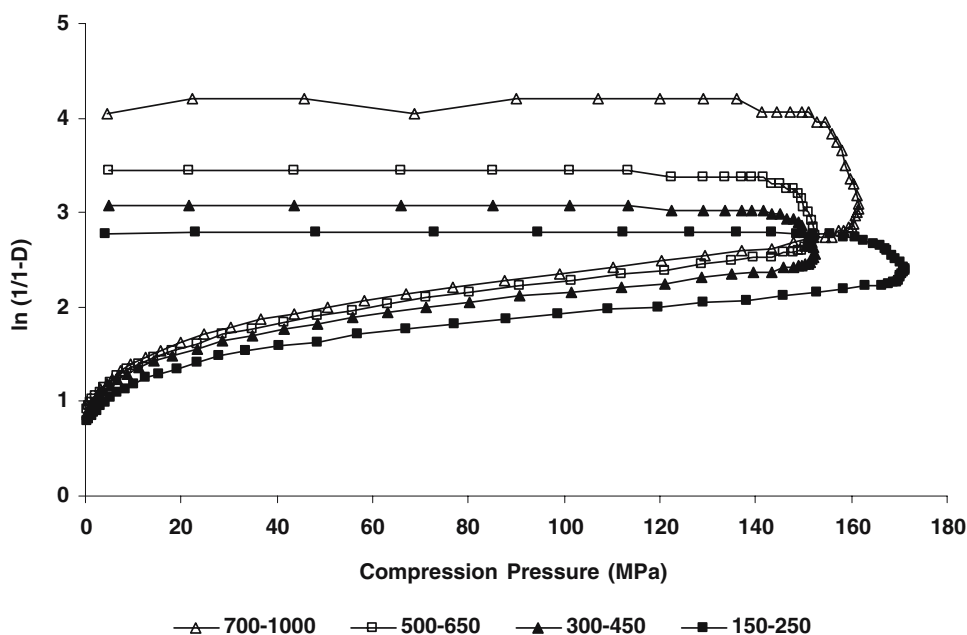
Fig. 2. In-die Heckel plots for four size fractions of paracetamol compressed at 8.6 ± 0.3 kN. Initial curvature at low pressure (0–25 MPa) corresponds to particle rearrangement, while the linear part of the curve indicates the ability of the material to deform plastically (25–90 MPa). At higher pressures curvature was observed due to strain hardening (work hardening). In-die elastic expansion after removal of force leads to decompression phase of Heckel plot.

Adams Analysis

The Adams equation (2) is a derived model to estimate the fracture strength of a single granule from in-die compression data. It models the bed of granules in the die as a series of parallel load-bearing columns and gives the stress and natural strain relationship.

$$\ln P = \ln \left(\frac{\tau_0{}'}{\alpha'} \right) + \alpha'\varepsilon + \ln \left(1 - e^{(-\alpha'\varepsilon)} \right) \qquad (10)$$

where, P is the applied pressure and ε is the natural strain which is given by:

$$\varepsilon = \ln(h_0/h) \qquad (11)$$

where, h_0 and h are the initial and current heights of the bed, respectively. The quantity $\tau_0{}'$ is the apparent single agglomerate strength which is related to the actual strength, τ_0 as follows:

$$\tau_0{}' = K_1\tau_0 \qquad (12)$$

where, K_1 is a constant. The quantity α' is related to friction between particles.

At higher values of natural strain, the last term of Adams equation (Eq. 10) becomes negligible and can be omitted, leaving a linear function. As per the Adams equation, graphic transformation of stress–strain relationship showed linearity over whole pressure range with good correlation coefficient values ($R^2 > 0.99$). Intercept and slope values obtained from linear regression analysis between $\ln P$ and natural strain were used to calculate $\tau_0{}'$. Adams' $\tau_0{}'$

values increased with decrease in particle size and increased at increased applied pressure (Table III).

Elastic Deformation

Elastic recovery is the reversible part of deformation, and is indicative of poor interparticulate bonding. Paracetamol tablets from each fraction of particle size were too weak and capped after ejection, which made it difficult to measure tablet thickness outside the die. Therefore, in-die tablet thickness was calculated using data obtained from upper and lower punch displacement. The percentage axial elastic recovery (ER) was calculated using equation described by Armstrong and Haines-Nutt (28).

$$\%ER = [(H - Hp)/Hp] \times 100 \qquad (13)$$

where, Hp and H are the thickness of tablet under maximum pressure and after the compression force was removed, respectively. From the results of elastic recovery of each particle size fraction, it was shown that as the compression force was increased, the elastic recovery also increased (Table II). Particle size also had a significant influence on the elastic recovery, with a higher elastic recovery observed for larger size particles than smaller size particles.

Another way to express the elastic property of material is to obtain the ratio of elastic energy (EE) to plastic energy (PE). PE and EE represent the "good" and "bad" parameters, respectively, of the overall compactability. PE and EE were calculated from force displacement compaction profile (24,29). The data of EE/PE from Table II indicates that as

Table III. Walker Parameter (Pressing Modulus, L) for Different Particle Size Fractions at Three Different Compression Forces from the Linear Regression Analysis (at pressure ranges shown) of Transformation log P vs. $1/D$ ($R^2 > 0.991$)

Compression force (kN)	Particle size (µm)	Pressing modulus, L	Linear part for L (MPa)	Compressibility coefficient, W	a	$1/b$ (MPa)	Linear part for Kawakita equation (MPa)	Adams τ_0' values (MPa)	Linear part for Adams equation (MPa)
5.2 (0.4)	700–1,000	0.839 (0.0009)	1–90	25.6 (0.262)	0.424 (0.005)	9.12 (0.5)	18–100	11.6 (0.8)	1–95
	500–650	0.816 (0.0001)	1–105	25.8 (0.154)	0.418 (0.001)	10.6 (0.8)	19–111	15.4 (0.2)	2–100
	300–450	0.799 (0.0001)	1–97	27.5 (0.24)	0.414 (0.005)	11.5 (0.7)	17–107	16.6 (0.1)	1–90
	150–250	0.785 (0.00005)	1–104	28.7 (1.19)	0.401 (0.007)	13.9 (1.1)	15–99	19.0 (0.3)	1–97
8.6 (0.3)	700–1,000	0.803 (0.0001)	2–165	24.9 (0.111)	0.416 (0.004)	12.0 (0.01)	19–161	14.5 (1.1)	1–160
	500–650	0.801 (0.0083)	2–156	25.1 (0.254)	0.403 (0.001)	12.8 (0.02)	20–173	15.3 (0.2)	2–168
	300–450	0.786 (0.0001)	5–178	27.2 (0.151)	0.403 (0.001)	13.2 (0.04)	18–158	16.2 (1.7)	1–180
	150–250	0.782 (0.00001)	1–180	28.0 (0.343)	0.400 (0.005)	17.7 (1.5)	16–165	19.7 (0.6)	2–176
17.3 (1.6)	700–1,000	0.830 (0.0001)	20–124	24.2 (0.23)	0.384 (0.005)	16.3 (1.8)	20–322	17.8 (3.4)	2–269
	500–650	0.800 (0.0001)	11–119	25.1 (0.238)	0.393 (0.008)	12.7 (2.1)	15–315	19.6 (3.0)	1–258
	300–450	0.774 (0.0001)	15–147	28.4 (0.155)	0.418 (0.006)	16.9 (2.9)	18–289	21.4 (2.7)	1–276
	150–250	0.755 (0.0004)	12–121	29.4 (0.26)	0.426 (0.008)	15.8 (2.3)	17–305	26.3 (3.8)	1–271

Compressibility coefficient (W) was calculated from the linear regression transformation of $100V$ *versus* log P between pressure range 5–125 MPa ($R^2 > 0.989$). Kawakita parameter a and $1/b$ were obtained from linear regression ($R^2 > 0.9979$) of P/C *versus* P. Adams parameter τ_0 was obtained from linear regression of ln P *versus* ε ($R^2 > 0.9947$). Linear parts of the Kawakita and Adams equations used to calculate respective parameters are also shown. Each value represents average of six tablet measurements with their standard deviations in parenthesis.

the compression force was raised, tablets made from different fractions of paracetamol showed increased tendency to undergo elastic deformation. For a given compression force, smaller sized particles underwent lesser elastic deformation, than larger sized particles.

DISCUSSION

This study investigated the effect of particle size based mechanical properties and compression force on parameters derived from various mathematical models in confined compression loading. Attempt was made to compare Heckel, Kawakita, and Adams parameters with each other and with single particle fracture strength. Although, the various mathematical models are based on different assumptions and transformations, they all provide indications of compressibility. We have therefore, examined the inter-relationship between these mathematical parameters and how these get affected by independent variables of particle size and compression force.

Heckel Analysis

Lower values of D_a, D_0 and D_b for smaller sized particles (lower propensity towards particle rearrangement/fragmentation) are due to presence of larger number of contact points per unit area and increased frictional and cohesive forces at zero pressure which oppose dense packing and relative particle rearrangement at low force. Low fragmentation tendency at a given pressure for smaller sized particles can also be explained by higher nominal fracture strength observed for smaller size particles in micro tensile testing. However, at higher compression force, there was no observable trend in the values of D_a, D_0 and D_b. This is attributed to the fact that extensive fragmentations at higher force nullify the effect of initial particle size on particle rearrangement and on the compressibility. The fragmentation of larger particles (at initial stage) produces small particles which serve a void filling role. The void filling role of fragmented particles increases the relative density of the in-die tablet.

Figure 2 shows the plot of the measured compression pressure as a function of relative density. It shows elasto-plastic deformation and fracture characteristics (0–25 MPa). The linear region (25–90 MPa) corresponds to the apparent mean yield pressure of the particles undergoing compaction. It is clearly observed that part of the curve is linear as per the Heckel equation.

Values of mean yield pressure obtained from Heckel plot depend on viscoelastic (plastic, and elastic) and fragmentation properties of the material (30–32). It is difficult to quantify viscoelastic behavior (plastic and elastic) of material from the linear regression of the Heckel plot (14,32,33). To distinguish between plastic and elastic deformation phenomenon, Deburg and Nystrom divided the Heckel plot into compression and decompression phases (32). Elastic deformations of the particles during decompression phase increases the porosity and reduces the relative density. In the absence of elastic deformation (negligible elastic expansion of tablet), decompression phase should be approximately horizontal. A significant deviation in decompression phase

from horizontal, as in present study indicates elastic behavior under pressure; translating into a low mean yield pressure. As shown in Fig. 2, the in-die Heckel plots for largest particle size fractions of paracetamol show greatest deviations from horizontality in the decompression region. This is indicative of higher degree of elastic deformation for larger particles during decompression phase. Therefore, the low value for Py for larger particle size of paracetamol is an indication of elastic deformation rather than only plastic deformation.

The Py obtained from linear regression analysis of Heckel plot was roughly linear to the Young's modulus for different size of particles (Fig. 3a). Young's modulus represents the stress–strain relation and is used as a measure of elastic properties of the materials; therefore it is likely that yield pressure equally reflects the effect of Young's modulus of the particles. The results of elastic recovery and elastic energy to plastic energy ratio show that excess input of energy (in the form of compression force) is utilized as elastic recovery in each particle size fraction indicating elastic deformation under pressure. Force dependent increase in elastic deformation is due to inability of paracetamol to relieve stress and further undergo plastic deformation. This is attributed to the high elastic nature of the paracetamol with very poor interparticulate bonding. Also, very negligible elastic recovery was observed at compression force of 4.8 kN. This is an evidence of stress dependent elastic recovery of paracetamol. At the highest studied compression force of 17.3 kN, the standard deviation in the values of Young's moduli and elastic recovery were on the higher side, although the trend in the mean values of the two parameters was intact for all particle size fractions. This can be explained as a case of non-equilibrium between stress and strain at very high compression force, leading to higher variability in the calculated parameters. The lower elastic recovery of the smaller size particle can be attributed to more homogenous pore distribution which provides more plasticity and less elasticity. The number of contacts points per unit area in case of smaller size particle also gives substantially more interparticulate interaction.

It was observed that elastic recovery was linearly related to Py for each of the particle size fractions at all compression forces studied (Fig. 3b). In order to elucidate the effect of elastic and plastic deformation on the apparent mean yield pressure, elastic to plastic energy ratio (EE/PE) was calculated from force–displacement compression profile. EE/PE of each of particle size fraction at each compression force was found to be linearly proportional to Py (Fig. 3c), which further indicated that elastic deformation under pressure influences the calculated values of Py. In the Heckel model, it is assumed that the voidage variation after particle rearrangement is only due to plastic deformation. It is therefore clear that Py does not represent the yield stress of particles due to plastic deformation, and the decrease of voidage is mainly caused by particles rearrangement and elastic deformation.

To probe the pressure dependency of the apparent mean yield pressure, each set of powder bed was compressed at three different compression forces. Results indicated that for any given fraction of paracetamol, as the compression force increased, apparent mean yield pressure increased (Fig. 4). Rees and Konkel had also reported the pressure dependency
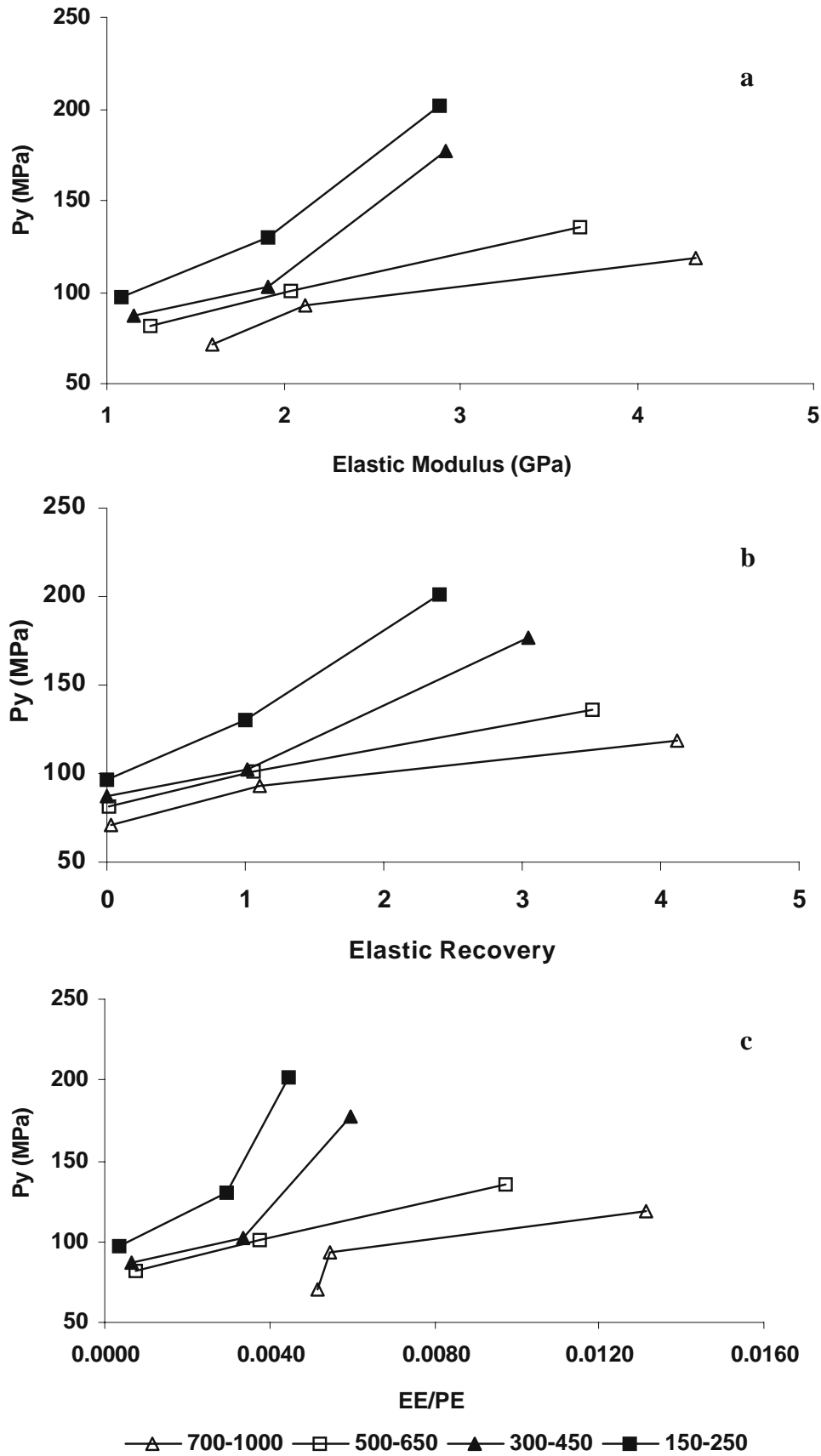
Fig. 3. Apparent Mean Yield Pressure, Py *vs.*: (a) Young's modulus, (b) Elastic recovery, and (c) *EE/ PE* ratio from compression of four different size particles compressed at three different forces.

of the apparent mean yield pressure (34,35). Heckel analysis does not accurately describe the compaction of pharmaceutical powders at high compaction pressures, because small error in determination of relative density might cause significant error in the logarithmic transformations. This fact is also apparent in Fig. 4 where a greater scatter was observed at higher applied force as compared to lower forces.

Walker Analysis

Walker analysis for various combinations of particle size and compression force was carried out from linear regression analysis of log P *vs.* $1/D$. Values of pressing modulus increase as the particle size increased (Table III), indicating a smaller change in volume for a given pressure, in case of the larger particles. This is due to closer initial particle packing with minimum void space in smaller particles resulting in larger volume change. The compressibility coefficient, W which describes the percentage change in volume on logarithmic scale of applied pressure increased for decrease in particle size. The higher change in volume in case of smaller sized particles can be attributed to lower observed initial porosities or lower voids space. As opposed to the Heckel parameter, (Py) Walker parameters of pressing modulus and the compressibility coefficient do not show pressure dependency. The pressure dependent discrimination of Heckel and Walker parameters is explained by the fact that the Heckel transformation is practically linear at low densities corresponding to the well-known lack of fit at low pressures while the Walker transformation is most curved in this region. At high densities, the Walker equation approximates linearity while the Heckel transformation tends to infinity (13). From the comparative assessment of Heckel and Walker models under the conditions studied, it can be concluded that Heckel model has lesser discriminative

power, because the elastic deformation and the applied pressure greatly influence the Heckel parameter.

Kawakita Analysis

Kawakita parameter a describes the initial porosity at zero pressure which corresponds to the total portion of reducible volume at maximum pressure. The values of a decreased as the particle size decreased due to relatively closer packing arrangement in case of smaller sized particles. This can be explained by the fact that nearer to theoretical spherical shape crystal habit facilitates efficient packing in case of smaller size particles. As with the pressing modulus from Walker equation, parameter a also describes the relative volume reduction at maximum pressure. From the values of pressing modulus and the a parameter, a consistent trend can be seen between two parameters, especially at 5.2 and 8.6 kN compression force. However, considering the pressure dependency of Kawakita model, the trend was lost at the highest force (17.3 kN).

The higher value of $1/b$ indicates that a higher force is required to reduce a volume to half of its original. The greater force required to reduce the volume to one half for the smaller sized particles can be attributed to a larger surface area, greater contact points, and a higher cohesion and frictional force. This corresponds to higher nominal fracture strength of particle obtained from micro tensile testing. The particles formed upon fragmentation from larger particles are always smaller in size and thereby yield at a higher pressure. Additionally, more surface area available for larger particles easily initiates crack propagation when tested under load as compared to smaller sized particles. A good co-relationship (Table IV) was seen to exist between $1/b$, and Py derived from Heckel plot, and also between $1/b$ and nominal strength of individual particles at 5.2 and 8.6 kN, indicating
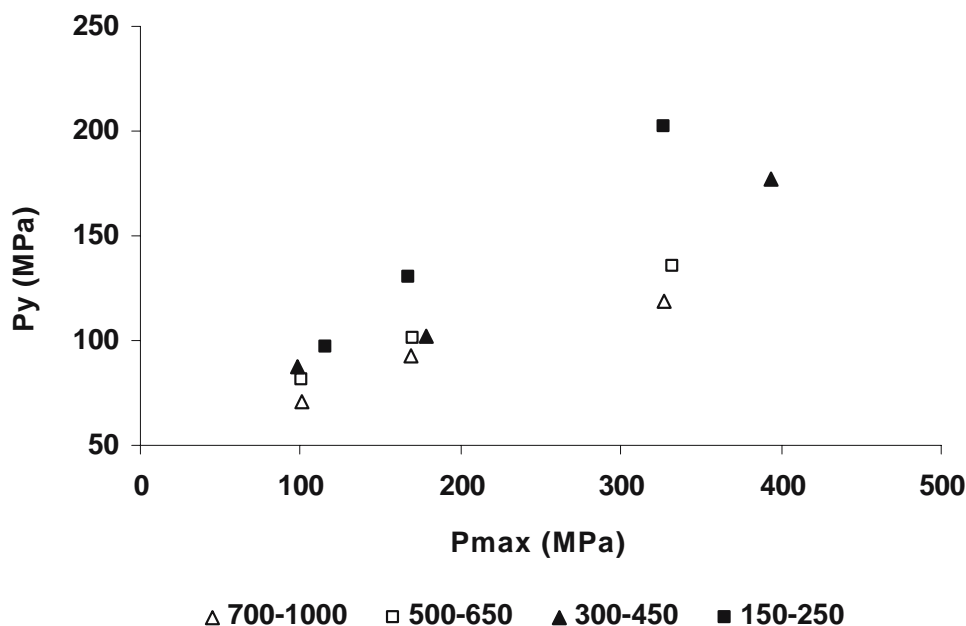

Fig. 4. Relationship between maximum pressure, Pmax and the apparent yield pressure (Py) for four particle size fractions. Values of Py linearly increased with applied pressure for all four particle sizes.

Table IV. Observed Inter Relationship between the Nominal Fracture Strength (τ_{0s}) Derived from Single Particle Fracture and the In-die Measurement of Yield Strength by Heckel (Py), Kawakita (1/b), and Adams Equations (τ_0') Using Four Different Particle Size Fractions in Confined Compression at Three Compression Forces

Compression Force (kN)	$Py \rightarrow 1/b$ $(Y \rightarrow X)$	$Py \rightarrow \tau_0'$ $(Y \rightarrow X)$	$1/b \rightarrow \tau_0'$ $(Y \rightarrow X)$	$\tau_{0s} \rightarrow Py$ $(Y \rightarrow X)$	$\tau_{0s} \rightarrow 1/b$ $(Y \rightarrow X)$	$\tau_{0s} \rightarrow \tau_0'$ $(Y \rightarrow X)$
5.2 (0.4)	$Y = 5.3724X + 23.601$	$Y = 3.5455X + 28.703$	$Y = 0.6321X + 1.3849$	$Y = 0.0732X^2 - 10.789X + 400.2$	$Y = 1.2943X^2 - 21.543X + 91.623$	$Y = 1.1594X^2 - 30.164X + 197.18$
	$R^2 = 0.9719$	$R^2 = 0.9867$	$R^2 = 0.9313$	$R^2 = 0.9999$	$R^2 = 0.9939$	$R^2 = 0.9987$
8.6 (0.3)	$Y = 6.3701X + 17.558$	$Y = 7.0824X - 10.131$	$Y = 1.1066X - 4.2614$	$Y = -0.0036X^2 + 1.8702X - 40.67$	$Y = -0.6556X^2 + 26.529X - 222.18$	$Y = 3.8965X^2 - 125.96X + 1011.1$
	$R^2 = 0.9967$	$R^2 = 0.9905$	$R^2 = 0.9845$	$R^2 = 0.9743$	$R^2 = 0.9785$	$R^2 = 0.9985$
17.3 (1.6)	[a]	$Y = 9.9129X - 52.624$	[a]	$Y = 0.0077X^2 - 2.0302X + 137.6$	[a]	$Y = 0.2292X^2 - 5.459X + 27.316$
		$R^2 = 0.9055$		$R^2 = 0.9768$		$R^2 = 0.9957$

[a] Poor correlation was found between the mathematical parameters.

that $1/b$ has the discriminative power to describe yield strength of materials. However, at highest studied compression force (17.3 kN), poor curve fitting was obtained due to pressure dependence of Kawakita parameter. The nonlinearity in the higher pressure range is because materials undergoing compaction affect the pressure course in such a way that porosity or relative volume estimation may be wrong at very high applied pressures. This fact can also be interpreted as the increase in the resistance against compression of total powder bed leading to high elastic expansion of the compact, thereby affecting the relative volume. When mathematically comparing Heckel and Kawakita Equations, volume terms in Kawakita equation can be transformed into porosity and relative density by considering the true density and compacted mass of the powder bed leading to a Heckel like transformation. Kawakita equation therefore can be
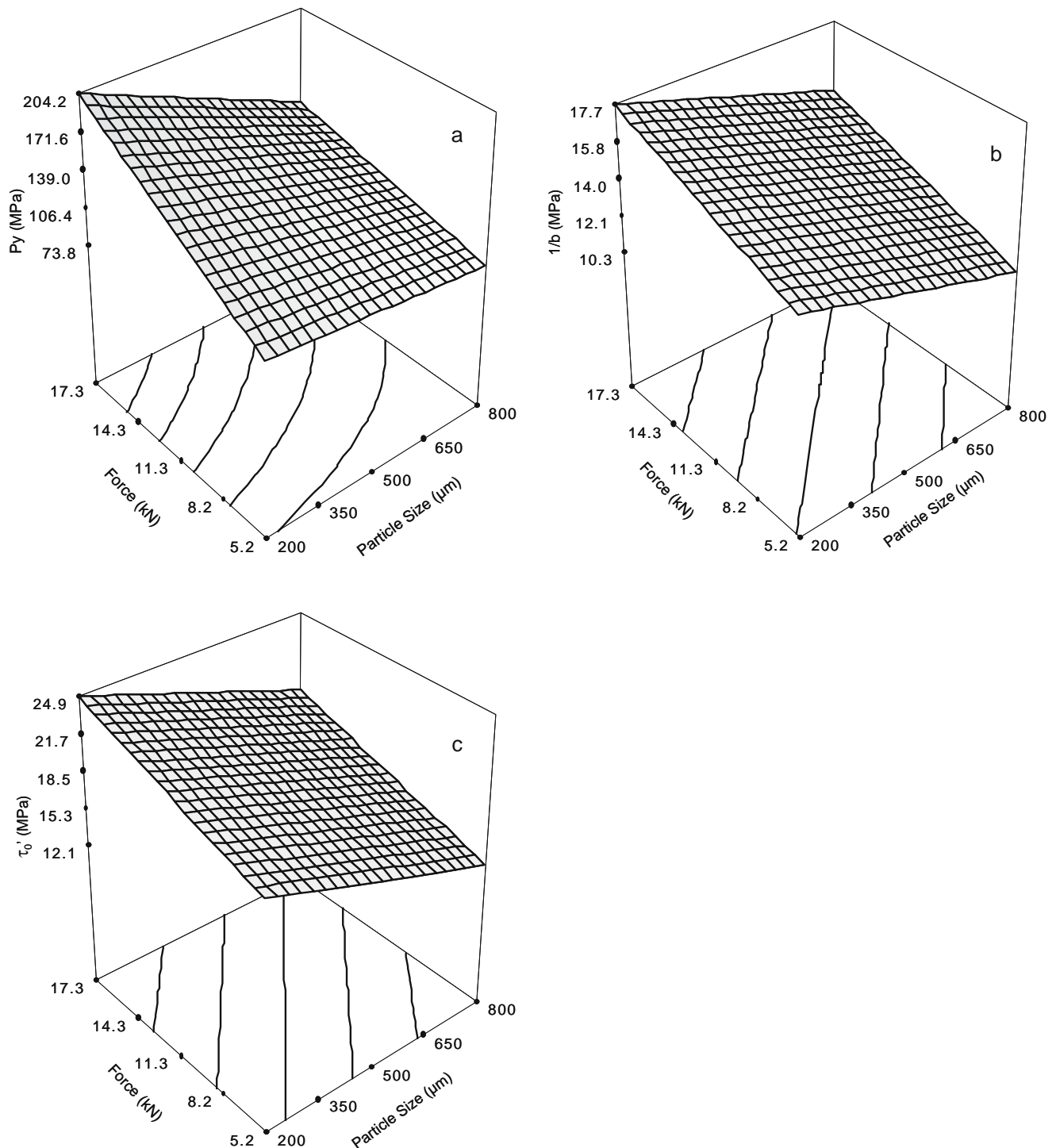
Fig. 5. Response surface plot eliciting the effect of particle size and applied force on (a) Heckel parameter, (b) Kawakita parameter, and (c) Adams parameter.

regarded as a special case of more general Heckel equation (36). Like Heckel parameters, the Kawakita parameters (a and $1/b$) also show pressure dependency. In fact, the constant in the Heckel equation, which only involves the yield strength of the material, is replaced by a term that involves the initial porosity.

Adams Analysis

The transformation as per Adams equation from stress–strain relationship showed linearity over the pressure range with good correlation coefficient values. The quantity, τ_0' describes the apparent single agglomerate strength, and the found values show that smaller particles have higher yield strength as compared to larger particles. Comparing the values of initial porosity from Kawakita equation (a), with Adams τ_0' values, a trend of decrease in τ_0 value with increase in powder initial porosity was observed at compression force of 5.2 and 8.6 kN. There was a good correlation between τ_0' and $1/b$; and between τ_0' and Py obtained for each particle size fraction (Table IV). However, as compared to $1/b$ and Py, the Adams parameter (τ_0') showed less pressure dependency. The values of nominal fracture strength of individual particles from micro tensile testing are consistent with the values obtained from bed compression Adams parameter. Adams et al. suggested that the Kawakita parameter ($1/b$) is less affected by the die wall friction during compression than Adams parameter (37). Since all experimental set ups used in the present study were used at constant die fill volume at one bed height, it also explains the effect of friction on the parameters. The results reported by Nicklasson (using microcrystalline cellulose and dicalcium phosphate agglomerates) were based on agglomeration failure process under load occurring by shearing deformation (15). Therefore, in powder volume reduction, either by fragmentation or deformation, the values of both single particle nominal fracture strength (τ_{0s}) and Adams parameter increased.

Inter-Relationships between the Studied Parameters

The relationship between the dependent and independent variables was illustrated using response surface plots. Response surface plot eliciting the effect of particle size and compression force (independent variables) and their interaction on cumulative response of Py, $1/b$, and τ_0' (dependent variables) are shown in Fig. 5. It is observed that at 5.2 and 8.6 kN compression force no pressure dependency was observed as compared to 17.3 kN force, where results were influenced by applied force. ANOVA for response surface linear model was found to be significant ($P > 0.01$) for all mathematical parameters. The theoretical (predicted) values and the experimental (observed) values were in close agreement in range studied. Regression equations were derived to predict the response of dependent variables due to quantitative effect of independent variables (particle size (PS) and compression force (F)).

$$Py = 96.16 - 0.083PS + 6.08F \tag{14}$$

$$1/b = 13.51 - 0.006PS + 0.31F \tag{15}$$

$$\tau_0' = 18.94 - 0.012PS + 0.48F \tag{16}$$

Additionally, linear correlation between the parameters derived from Heckel, Kawakita, and Adams equations was obtained (Table IV). Again, accounting for the force dependency of Heckel and Kawakita models, linearity exist at 5.2 and 8.6 kN, while at 17.3 kN, the correlation coefficient was poor. To relate the independent variables in this study, particle size, and compression force; with the dependent variables, viz. Py, $1/b$, τ_0', and τ_{0s}, a polynomial regression was attempted. Second order polynomial equations to describe the relationship are listed in Table IV. Results indicated that values obtained from mathematical transformations were valid for 5.2 and 8.6 kN compression forces except in case of Kawakita parameter ($1/b$), where at higher compression force (17.3 kN) correlation coefficient was poor. As with the interaction between independent variables, the impact of X on Y can be significant at some values of X and non-significant at other values. This is based on the fact that this polynomial represents a conditional relationship. The inclusion of the polynomial allows for the effect X on the dependent variable to vary based on the value of X. Heckel and Adams parameters showed relationship with nominal single particle fracture strength at all three forces.

CONCLUSION

This investigation attempted the study of compaction behavior of paracetamol using different particle sizes at varying compression forces. Heckel, Walker, Kawakita, and Adams model data fitting of compression was employed in addition to the micro tensile testing and quantification of elastic property. Heckel's parameter (Py) was influenced by elastic deformation under force, and therefore, the Heckel analysis does not have general validity and should be used with caution. The Heckel's parameter (Py) and Kawakita parameter ($1/b$) showed pressure dependency due to elastic deformation and wrong estimations of porosity at higher pressure, respectively. This calls for a critical assessment of the in-die and out-die Heckel plots by considering the fundamental deformation behavior of the materials under question. The parameters derived from Walker, Kawakita, and Adams equation varied with applied pressure and initial porosity. Walker and Adams parameters, however, showed no pressure dependency over the range studied. The nominal fracture strength from micro tensile testing was shown to be related to the parameters obtained from Heckel, Walker, Kawakita and Adams in confined compression of bulk material. The single particle strengths derived from the whole bed deformation curves, agreed in value with the strengths found on individual particles and allowed a physical interpretation to be made from the $1/b$ parameter in the Kawakita equation.

In tablets with low dose drugs, compaction properties are overshadowed by the encouraging compaction behavior of commonly used excipients. However, in case of high dose drugs, inherent compaction of the drug assume greater critically for the overall success of compression process. Particle size distribution of drug, granulation technique, and rate and magnitude of applied force—influence the tableting

attributes. An obvious extrapolation of this study should be to investigate the effect of excipients with different compression characteristics on the compaction behavior of formulation matrix containing high dose drugs. Moreover, the role of drug particle size distribution and compression force in the presence of excipients should be studied for such a system. A formulation development protocol, incorporating the above parameters can help in selection of excipients, optimization of manufacturing process, and identification of critical process parameters, thereby facilitating successful transfer of technology to the production stage.

ACKNOWLEDGMENTS

REFERENCES

1. H. Rumpf. The strength of granules and agglomerates. In W. A. Knepper (ed.), *Agglomeration*, Interscience, London, 1962, pp. 379–418.
2. M. J. Adams, M. A. Mullier, and J. P. K. Seville. Agglomerate strength measurement using a uniaxial confined compression test. *Powder Technol.* **78**:5–13 (1994).
3. E. E. Walker. The properties of powder. Part VI. The compressibility of powders. *Trans. Faraday Soc.* **19**:73–82 (1923).
4. I. Shapiro. Ph.D. Thesis, University of Minnesota (1944).
5. R. W. Heckel. Density–pressure relationships in powder compaction. *Trans. Metall. Soc. AIME* **221**:671–675 (1961).
6. R. W. Heckel. An analysis of powder compaction phenomena. *Trans. Metall. Soc. AIME* **221**:1001–1008 (1961).
7. K. Kawakita and K. H. Lüdde. Some considerations on powder compression equations. *Powder Technol.* **4**:61–68 (1971).
8. K. Kawakita, I. Hattori, and M. Kishigami. Characteristic constants in Kawakita's powder compression equation. *J. Powder Bulk Solids Technol.* **1**:3–8 (1977).
9. P. Paronen. Using Heckel equation in the compression studies of pharmaceuticals. In *Proc. 4th Int. Conf. Pharmaceutical Technology*, Paris 301–307 (1986).
10. R. J. Roberts and R. C. Rowe. The compaction of pharmaceutical and other model materials—a pragmatic approach. *Chem. Eng. Sci.* **42**:903–911 (1987).
11. C. M. Gabaude, M. Guillot, J. C. Gautier, P. Saudemon, and D. Chulia. Effects of true density, compacted mass, compression speed, and punch deformation on the mean yield pressure. *J. Pharm. Sci.* **88**:725–730 (1999).
12. J. M. Sonnergaard. Impact of particle density and initial volume on mathematical compression models. *Eur. J. Pharm. Sci.* **11**:307–315 (2000).
13. J. M. Sonnergaard. A critical evaluation of the Heckel equation. *Int. J. Pharm.* **193**:63–71 (1999).
14. A. Hassanpour and M. Ghadiri. Distinct element analysis and experimental evaluation of the Heckel analysis of bulk powder compression. *Powder Technol.* **141**:251–261 (2004).
15. F. Nicklasson and G. Alderborn. Analysis of the compression mechanics of pharmaceutical agglomerates of different porosity and composition using the Adams and Kawakita equations. *Pharm. Res.* **17**:949–954 (2000).
16. L. E. Holman. The compaction behavior of particulate materials. An elucidation based on percolation theory. *Powder Technol.* **66**:265 (1991).
17. W. Chen and S. G. Malghan. Investigation of compaction equations for powders. *Powder Technol.* **81**:75–81 (1994).
18. R. Panelli and A. Filho. A study of a new phenomenological compacting equation. *Powder Technol.* **114**:255–261 (2001).
19. J. M. Sonnergaard. Investigation of a new mathematical model for compression of pharmaceutical powders. *Eur. J. Pharm. Sci.* **14**:149–157 (2001).
20. K. M. Picker. A new theoretical model to characterize the densification behavior of tableting materials. *Eur. J. Pharm. Biopharm.* **49**:267–273 (2000).
21. J. S. M. Garr and M. H. Rubinstein. An investigation into the capping of paracetamol at increasing speeds of compression. *Int. J. Pharm.* **72**:117–122 (1991).
22. O. F. Akande, M. H. Rubinstein, P. H. Rowe, and J. L. Ford. Effect of compression speeds on the compaction properties of a 1:1 paracetamol–microcrystalline cellulose mixture prepared by single compression and by combinations of pre-compression and main-compression. *Int. J. Pharm.* **157**:127–136 (1997).
23. E. Joiris, P. MartinoDi, C. Berneron, A. M. Guyot-Hermann, and J. C. Guyot. Compression behavior of orthorhombic paracetamol. *Pharm. Res.* **15**:1122–1130 (1998).
24. R. J. Oates and A. G. Mitchell. Calculation of punch displacement and work of powder compaction on a rotary tablet press. *J. Pharm. Pharmacol.* **41**:517–523 (1989).
25. C. Matz, A. Bauer-Brandl, T. Rigassi, R. Schubert, and D. Becker. On the accuracy of a new displacement instrumentation for rotary tablet presses. *Drug Dev. Ind. Pharm.* **25**:117–130 (1999).
26. M. Haisa, S. Kashino, R. Kawai, and H. Maeda. The monoclinic form of p-hydroxyacetanilide. *Acta Crystallogr. B.* **32**:1283–1285 (1976).
27. P. Espeau, R. Ceolin, J. L. Tamarit, M. A. Perrin, J. P. Gauchi, and F. Leveiller. Polymorphism of paracetamol: relative stabilities of the monoclinic and orthorhombic phases inferred from topological pressure–temperature and temperature–volume phase diagrams. *J. Pharm. Sci.* **94**:524–539 (2005).
28. N. A. Armstrong and R. F. Haines-Nutt. Elastic recovery and surface area changes in compacted powder systems. *J. Pharm. Pharmacol.* **24**:135P–136P (1972).
29. O. Antikainen and J. Yliruusi. Determining the compression behavior of pharmaceutical powders from the force-distance compression profile. *Int. J. Pharm.* **252**:253–261 (2003).
30. P. York. Particle slippage and rearrangement during compression of pharmaceutical powders. *J. Pharm. Pharmacol.* **30**:6–10 (1978).
31. M. Duberg and C. Nystrom. Studies on direct compression of tablets XI. Evaluation of methods for the estimation of particle fragmentation during compaction. *Acta Pharm. Suec.* **19**:421–436 (1982).
32. M. Duberg and C. Nystrom. Studies on direct compression of tablets XVII. Porosity–pressure curves for the characterization of volume reduction mechanism in powder compaction. *Powder Technol.* **46**:67–75 (1986).
33. C. Sun and D. J. Grant. Influence of elastic deformation of particles on Heckel analysis. *Pharm. Dev. Technol.* **6**:193–200 (2001).
34. J. E. Rees and K. D. Tsardaka. Some effects of moisture on the viscoelastic behavior of modified starch during powder compaction. *Eur. J. Pharm. Biopharm.* **40**:193–197 (1994).
35. P. Konkel and J. B. Mielck. Associations of parameters characterizing the time course of the tableting process on a reciprocating and on a rotary tableting machine for high-speed production. *Eur. J. Pharm. Biopharm.* **45**:137–148 (1998).
36. P. J. Denny. Compaction equations: a compression of the Heckel and Kawakita equations. *Powder Technol.* **127**:162–172 (2002).
37. M. J. Adams and R. McKeown. Micromechanical analyses of the pressure–volume relationships for powders under confined uniaxial compression. *Powder Technol.* **88**:155–163 (1996).